

See discussions, stats, and author profiles for this publication at: <https://www.researchgate.net/publication/46254486>

Modulated Photophysics of an ESIPT Probe 1-Hydroxy-2-naphthaldehyde within Motionally Restricted Environments of Liposome Membranes Having Varying Surface Charges

ARTICLE *in* THE JOURNAL OF PHYSICAL CHEMISTRY B · OCTOBER 2010

Impact Factor: 3.3 · DOI: 10.1021/jp1048138 · Source: PubMed

CITATIONS

39

READS

24

2 AUTHORS, INCLUDING:



Bijan Kumar Paul

Indian Institute of Science Education and ...

72 PUBLICATIONS 895 CITATIONS

SEE PROFILE

Modulated Photophysics of an ESIPT Probe 1-Hydroxy-2-naphthaldehyde within Motionally Restricted Environments of Liposome Membranes Having Varying Surface Charges

Bijan Kumar Paul and Nikhil Guchhait*

Department of Chemistry, University of Calcutta, 92 A. P. C. Road, Calcutta-700009, India

Received: May 26, 2010; Revised Manuscript Received: August 27, 2010

The present work demonstrates the modulation of excited state intramolecular proton transfer (ESIPT) emission of 1-hydroxy-2-naphthaldehyde (HN12) upon its interaction with the liposomal vesicles/bilayer of dimyristoyl-L- α -phosphatidylcholine (DMPC) and dimyristoyl-L- α -phosphatidylglycerol (DMPG) and its subsequent implementation as an efficient molecular reporter for probing of microheterogeneous environments of lipid-bilayer system. Modifications on the emission profile of HN12 in terms of remarkable emission intensity enhancement coupled with a hypsochromic shift induced by the presence of DMPC and DMPG membranes have been interpreted to be vivid manifestations of the interactions between the two partners. Steady-state anisotropy, red-edge excitation shift (REES), and time-resolved fluorescence measurements have been fruitfully exploited to complement other experimental findings. Probable binding site of HN12 in the lipid-bilayers has been assessed on the basis of intertwining the results of fluorescence quenching with other experimental results and is further substantiated from docking studies.

1. Introduction

Supramolecular chemistry has traditionally been connected to the problems of structure and stability of various macromolecules and noncovalent structural architectures such as DNA, proteins, and membranes that form the fundamental building blocks of living systems.¹ One of the most important supramolecular structures is the vesicles which are dynamic structures composed of amphiphiles forming bilayers that enclose a small amount of water within.^{1–3} Particularly, the synthetic vesicles have captured special attention on account of their ability to mimic biological membranes.³ Vesicles that are composed of natural phospholipids are termed “liposomes”, which serve as models for biological membranes. Phospholipid bilayers constitute the matrix of natural membranes on which proteins, enzymes, and drugs display their activities.⁴ The complicated structure of natural biological membranes have always invited research in line of using synthetic liposome that mimic the structure and geometry of cell membranes.^{5,6} Apart from this, the diversity of the application of liposome also extends to the fields of drug loading, food industry, immunology, and so forth.

Recent time has witnessed a marvelous evolution of research in the field of membrane biochemistry regarding interaction of drug molecules with lipid membranes.^{7–10} Important issues like characterization of interaction behavior and location of the probe in the membrane have been addressed by various techniques of which fluorescence spectroscopy is one of the most extensively used ones.^{5,6,11–13} Penetration of the probe molecule into the hydrophobic/hydrophilic core of the bilayer will necessarily accompany ample alterations of its immediate surroundings (mainly by offering an atmosphere of varied polarity, viscosity, and imparting rigidity to rotational and vibrational degrees of freedom of the probe) and thereby leading to modified photophysics with respect to that in pure homogeneous fluids.

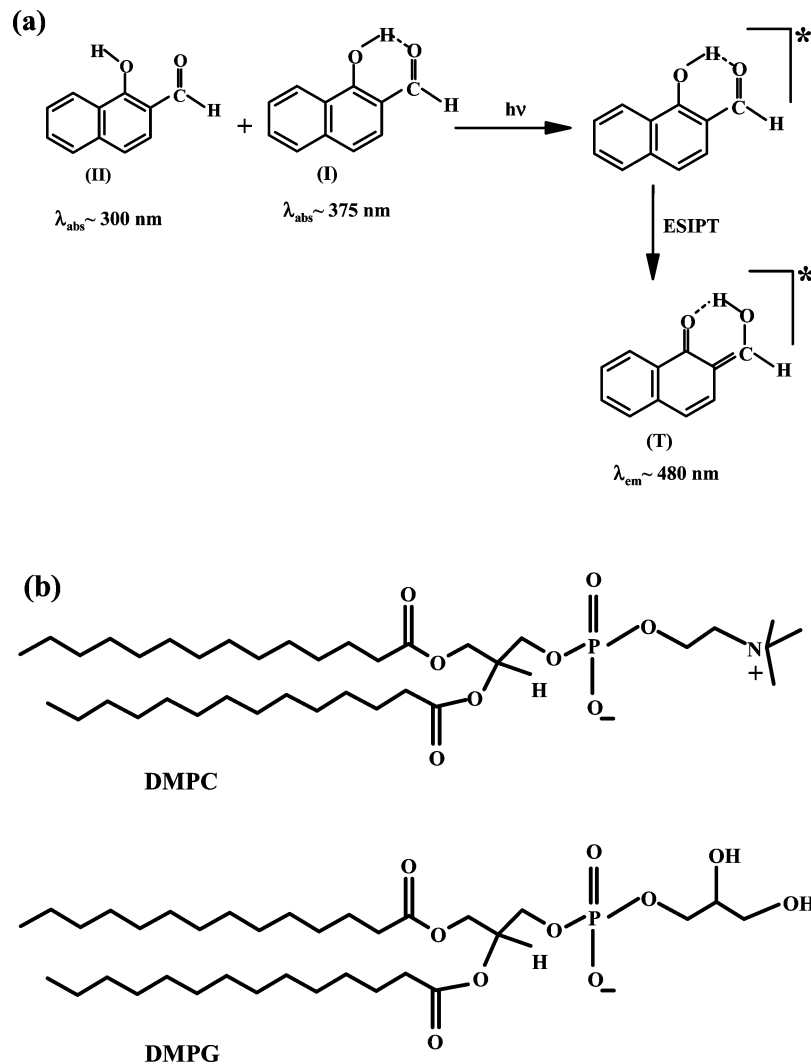
Important information can thus be collected by characterizing the nature and magnitude of modulations of photophysics of the probe.

Ever since the first report by Weller,¹⁴ the phenomenon of excited-state intramolecular proton transfer (ESIPT) reaction continues to receive immense attention even today. This is not only because of its unique photophysics, but also with a view to the viable expansion of the phenomenon in applicative research. The ESIPT probes have been applied in important areas like development of UV filters,¹⁵ proton transfer laser,^{16,17} photostabilizers,¹⁸ white-light emitting diode,¹⁹ and so on. Apart from these, the application of the ESIPT process extends to utilization of suitable ESIPT probes as molecular reporter for probing of complex biological^{20–23} and biomimicking environments^{24,25} as well as a variety of supramolecular assemblies.^{24–29} With a view to such viable expansion of the phenomenon, we have carried out the present program which aims at establishing the efficiency of a simple, potent ESIPT probe, namely, HN12 in studying the microenvironments of lipid-bilayers of DMPC and DMPG through thorough spectroscopic characterization of its modified photophysics upon interaction with the lipids. Dramatic changes on the emission profile in form of intensity enhancement and shifting of emission wavelength provide evidence for binding interaction between the two parties. The results demonstrate the effect of lipid environments on stationary fluorescence and anisotropy and time-resolved fluorescence decay properties of the entrapped fluorophore. Additionally, docking study is performed to assess the binding location of the probe.

2. Experimental Section

2.1. Materials. The synthesis and purification procedure of HN12 (Scheme 1) has been described elsewhere.³⁰ It was repeatedly recrystallized from C₂H₅OH, and the purity of the compound was established on TLC plate. DMPC and DMPG (Scheme 1) were procured from Sigma-Aldrich, U.S.A. (with purity >99%), and used as received. Triple distilled water was

* To whom correspondence should be addressed. Tel.: 91-33-23508386. Fax: +91-33-2351-9755. E-mail: nguchhait@yahoo.com.

SCHEME 1: (a) Schematic Presentation of the ESIPT Process in HN12; (b) Structures of DMPC and DMPG

used for preparing all solutions. Tris buffer was purchased from SRL, India, and the solution (Tris-HCl buffer) of required pH (7.40) was prepared from this. All solvents (e.g., CHCl_3 and CH_3OH) used were of UV spectroscopic grade (Spectrochem, India).

2.2. Instrumentations and Methods. The absorption and emission spectra were acquired on Hitachi UV-vis U-3501 spectrophotometer and Perkin-Elmer LS-55 fluorimeter, respectively, with standard quartz cuvettes of 1 cm path length. During absorption and emission measurements, the scan rate was maintained at 200 and 300 nm/s, respectively. The concentration of HN12 was maintained at $2.0 \mu\text{M}$ (to eliminate the possibilities of aggregation and reabsorption) and pH at 7.40 throughout the study.

Steady-state fluorescence anisotropy was measured on Perkin-Elmer LS-55 fluorimeter. The steady-state anisotropy (r) is defined as^{11,12,29}

$$r = \frac{(I_{VV} - G \cdot I_{VH})}{(I_{VV} + 2G \cdot I_{VH})} \quad (1)$$

$$G = \frac{I_{HV}}{I_{HH}} \quad (2)$$

where I_{VV} and I_{VH} are the emission intensities when the excitation polarizer is vertically oriented and the emission polarizer is oriented vertically and horizontally, respectively. G is the correction factor.

Fluorescence lifetimes were obtained from a time-correlated single photon counting (TCSPC) spectrometer using nanoLED-07 (IBH, U.K.) as the light source at 375 nm to trigger the fluorescence of HN12.²⁹ The observed fluorescence intensities were fitted by using a nonlinear least-squares fitting procedure to a function ($X(t) = A + \sum_i B_i E(t') R(t - t') dt'$) comprising the convolution of the IRF ($E(t)$) with a sum of exponentials ($R(t) = \sum_{i=1}^N B_i \exp(-t/\tau_i)$) with pre-exponential factors (B_i), characteristic lifetime (τ_i), and a background (A). Relative contribution of each component was obtained from a triexponential fitting and is expressed by the following equation:

$$\alpha_n = \frac{B_n}{\sum_{i=1}^N B_i}$$

The mean (average) fluorescence lifetimes for the decay curves were calculated from the decay times and the relative contribution of the components using the following equation:^{11,12,29}

$$\tau_{\text{avg}} = \langle \tau_f \rangle = \frac{\sum_i \alpha_i \tau_i^2}{\sum_i \alpha_i \tau_i} \quad (3)$$

For time-resolved fluorescence anisotropy decay measurements, the polarized fluorescence decays for the parallel [$I_{||}(t)$] and perpendicular [$I_{\perp}(t)$] emission polarizations with respect to the vertical excitation polarization were first collected at the emission maxima of the probe. The anisotropy decay function $r(t)$ was constructed from these $I_{||}(t)$ and $I_{\perp}(t)$ decays using the following equation:^{11,31}

$$r(t) = \frac{I_{||}(t) - G \cdot I_{\perp}(t)}{I_{||}(t) + 2G \cdot I_{\perp}(t)} \quad (4)$$

The grating factor, G , was determined from long-time tail matching technique.³¹

Fluorescence quantum yield (Φ_f) was determined using anthracene ($\lambda_{\text{abs}} \sim 350$ nm and $\Phi_f = 0.27$ in CH_3OH) as the secondary standard in the following equation:^{11,29}

$$\frac{\Phi_S}{\Phi_R} = \frac{A_S}{A_R} \times \frac{(\text{Abs})_R}{(\text{Abs})_S} \times \frac{n_S^2}{n_R^2} \quad (5)$$

where Φ is quantum yield, “Abs” is absorbance, A is the area under the fluorescence curve, and n is the refractive index of the medium. Subscript “S” and “R” denote the corresponding parameters for the sample and reference, respectively.

All experiments have been performed at 303 K, unless otherwise specified, that is, the temperature was maintained well above the phase transition temperature of the lipid to avoid any complicacy arising from liposomal phase transition. During fluorescence quenching experiment addition of Cu^{2+} salt (from a stock solution in Tris-HCl buffer) was limited within 100 μL to ensure no significant volume change.

2.3. Preparation of Liposome and Its Labeling. Liposomes of DMPC/DMPG were prepared according to the literature procedure.³² Briefly, appropriate quantity of phospholipid was solubilized in 2:1 (v/v) chloroform/methanol ($\text{CHCl}_3/\text{CH}_3\text{OH}$), from which thin films were deposited on the inner walls of a small fusion tube under a stream of dry nitrogen. The resulted film was dried in a vacuum desiccator for 60 h at 4 °C. The film was then hydrated and swelled in Tris-HCl buffer (pH 7.40) followed by vortexing to disperse the lipid. The dispersion was then sonicated for 40 min using a sonicator (Bransonic 1510E-DTH). The resulted solution was then centrifuged (Spinwin MC-02) at 10000 rpm for 7 min to remove foreign particles, if any. The final solution was used as the stock solution of lipid from which the required sample solutions were prepared following usual procedure of dilution and adding appropriate quantity of the probe. After addition of the probe the solutions were left to equilibrate for 35 min. The equilibrated solutions were then used for spectral measurements. Only freshly prepared solutions were used during spectroscopic measurements. Solutions for spectral background correction were prepared the same way except that the probe was omitted.

The size and size distribution of the lipids were extracted from dynamic light scattering (DLS) experiment which conforms to the formation of small unilamellar vesicles in both cases. The results of DLS experiment are mentioned in the Supporting Information (Figure S1).

2.4. Docking Studies. Docking studies were performed with AutoDock 4.2 suite of programs that utilizes the Lamarckian Genetic Algorithm (LGA) implemented therein. For docking of HN12 with lipid-bilayer system, the required file (corresponding to the three-dimensional structure of HN12) for the ligand (HN12) was created through combined use of Gaussian 03W³³ and AutoDock 4.2³⁴ software packages. The geometry of HN12 was first optimized at DFT/B3LYP/6-31G** level of theory using Gaussian 03W suite of programs and the resultant geometry was read in AutoDock 4.2 software in compatible file format, from which the required file was generated in AutoDock 4.2. For DMPC lipid-bilayer, a system comprising of 72 molecules of DMPC phospholipid has been used from <http://people.ucalgary.ca/~tieleman/download.html>. Similarly, the DMPG lipid-bilayer structure was obtained from <http://www.charmm-gui.org/>. At the beginning of the docking study all water molecules were removed and hydrogens were added followed by computing Gasteiger charges, as required in Lamarckian Genetic Algorithm.³³ The grid size was set to 126, 126, and 40 along X-, Y-, and Z-axis with 0.375 Å grid spacing. The AutoDocking parameters used were as follows: GA population size = 150; maximum number of energy evaluations = 250000; GA crossover mode = two points. The lowest binding energy conformer was searched out of 35 different conformers for each docking simulation (HN12 + DMPC and HN12 + DMPG) and the resultant one was used for further analysis. The PyMoL software package was used for visualization of the docked conformations.³⁵

3. Results and Discussions

3.1. Interaction of HN12 with DMPC and DMPG Lipids.

The photophysical properties of HN12 have been reported in details elsewhere.³⁰ HN12 exhibits two prominent absorption bands at ~ 300 and ~ 375 nm which are assigned, respectively, to the open conformer (conformer **II**, Scheme 1) and the intramolecularly H-bonded closed conformer (conformer **I**, Scheme 1) of HN12. Upon photoexcitation, this closed conformer **I** undergoes rapid ESIPT reaction with the signature of large Stokes-shifted emission at ~ 480 nm (in aqueous medium) which is attributed to the ESIPT phototautomer (conformer **T**, Scheme 1) of conformer **I**. The emission band is actually a dual band of which the higher energy band at ~ 353 nm is due to open conformer **II** of HN12.³⁰

The absorption spectra of HN12 is found to be hardly modified by the presence of the lipids except for slight increase in absorbance with increasing lipid concentration. However, reasons for such changes are not fully rationalized from the absorption spectra. The present observations are found to qualitatively comply with absorption spectral response of HN12 upon interaction with proteins,²⁰ micelles^{20,29} and even cyclo-dextrin nanocavities.²⁹

The results of interaction of HN12 with DMPC and DMPG lipid-bilayers are more dramatically reflected on the emission profile. Figure 1 shows remarkable intensity enhancement of both the rotamer ($\lambda_{\text{em}} \sim 350$ nm) and the tautomer ($\lambda_{\text{em}} \sim 480$ nm) emission of HN12 with increasing lipid concentration (DMPC and DMPG). The extent of modulation is found to be comparatively greater for the tautomer emission than the rotamer emission, and the effect is even more prominently seen in

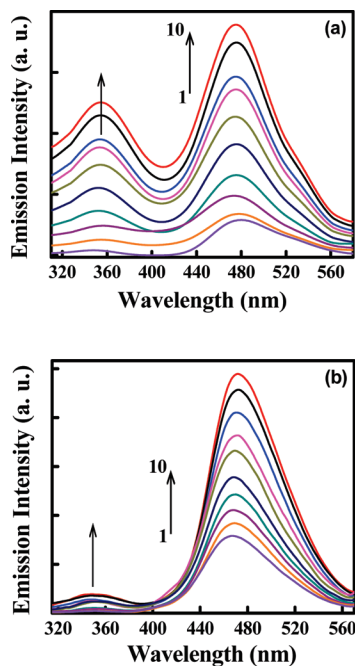


Figure 1. Emission spectra of HN12 as a function of increasing lipid concentration ($\lambda_{\text{ex}} = 300 \text{ nm}$). (a) Curves 1–10 correspond to [DMPC] = 0.0, 0.02, 0.05, 0.09, 0.30, 0.50, 0.70, 0.90, 1.50, 2.0 mM; (b) Curves 1–10 correspond to [DMPG] = 0.0, 0.02, 0.05, 0.09, 0.15, 0.25, 0.50, 0.80, 1.50, 2.0 mM.

DMPG lipid compared to DMPC. A close inspection of Figures 1 also reveals a slight blue shift of the emission maxima upon interaction with the lipids ($\Delta\lambda_{\text{em}}^{\text{max}} \sim 5 \text{ nm}$). Figures 2 produce a distinct reflection of the modifications to emission intensity and emission wavelength as a result of interaction with the liposome membranes. A steep rise of emission intensity is followed by attainment of a plateau region marking the saturation of interaction at $[\text{lipid}] \approx 0.90 \text{ mM}$.

The higher fluorescence quantum yield of HN12 in aprotic medium ($\Phi_f = 0.014$ in cyclohexane) compared to that in protic medium ($\Phi_f = 0.007$ in water) combined with the relative emission maxima positions ($\lambda_{\text{em}}^{\text{max}} \sim 475 \text{ nm}$ in cyclohexane versus $\lambda_{\text{em}}^{\text{max}} \sim 480 \text{ nm}$ in water)³⁰ produces clues to assess the nature and mechanism of interactions responsible for the observed modifications on emission spectral profile of HN12.^{7–10,20,29} A slight blue shift (Figures 2) coupled with fluorescence quantum yield enhancement (Φ_f of HN12 increases to 0.022 and 0.034 in 1.0 mM DMPC and DMPG, respectively) in lipid environments indicates that the polarity around the lipid-bound fluorophore is less than that in bulk aqueous phase (buffer medium). The blue shift is, however, not very large because of an intrinsic “intramolecular” nature of the ESIPT phenomenon

whence the emission properties (particularly the $\lambda_{\text{em}}^{\text{max}}$ position) of the external probe exhibit negligible medium-polarity dependence.³⁰

It is documented that liposome is a closed vesicle containing both hydrophobic and hydrophilic regions and depending on the nature of the probe it can penetrate into either the less polar region (toward the tail of the lipid) or into the polar part of the bilayer (toward the aqueous phase). Although HN12 has an overall neutral character (which may seem to promote its location into the hydrocarbon interior of the lipids^{20,29}), the presence of heteroatoms will impart an asymmetry in electronic charge distribution over the entire molecular framework. More importantly, the role of some specific interactions of the sort of hydrogen bonding, electrostatic interaction, and so on might be pivotal in governing the location of the extrinsic probe in lipids. However, it is too early to predict about the location of the extrinsic probe. The issue will be substantiated in forthcoming sections. Remarkable emission intensity enhancement of HN12 with increasing lipid concentration seems to be a manifestation of conjugate effects of reduced polarity of immediate vicinity of the fluorophore and substantial depletion of its radiationless decay channels as a result of restricted rotational and vibrational degrees of freedom when bound to the lipids. This assignment is consistent with previous reports from our group on interaction of HN12 with different biological, biomimicking, and supramolecular environments^{20,29} and also with a healthy score of literature reports.^{7,9,10,33} In the present case of investigation, a noticeable reduction of nonradiative decay rates in the lipid environments compared to that in the bulk aqueous buffer phase has been argued to be a major contributor to the observed emission intensity enhancement. The experimental results are presented and discussed in the forthcoming section.

3.2. Partitioning of HN12 in Lipid-Bilayers. Knowledge of the partitioning of the probe between the membrane environments to the aqueous phase is pertinent as well as important at this stage to have a quantitative estimation of the extent of penetration of the probe into the lipid-bilayer and also to realize the mechanism of interaction of the probe. The partition coefficient of the probe is defined as follows:³⁶

$$K_p = \frac{(C_m/C_t)/[\text{DMPC}]}{(C_w/C_t)/[\text{water}]} \quad (6)$$

where C_t is the total molar concentration of the probe and C_m and C_w stand for probes in lipid (DMPC or DMPG) and in water, respectively. Terms within square brackets represent molar concentration of respective species. The evaluation of partition coefficient of HN12 rests on an analysis of the fluorescence data on the basis of the following equation:^{7,36,38}

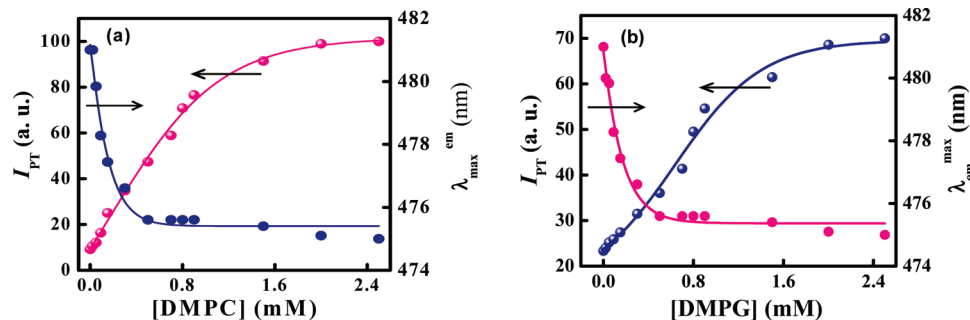


Figure 2. Variation of emission intensity and emission maxima of HN12 with increasing lipid concentration: (a) for DMPC and (b) for DMPG.

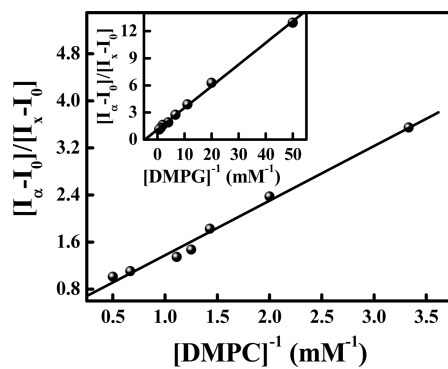


Figure 3. Plot of $(I_{\infty} - I_0)/(I_x - I_0)$ vs $[\text{lipid}]^{-1}$ (mM^{-1}) in lipid environments (DMPG in inset) using fluorescence data.

$$\frac{I_{\infty} - I_0}{I_x - I_0} = 1 + \frac{[\text{water}]}{K_p} \times \frac{1}{[\text{lipid}]} \quad (7)$$

in which I_0 , I_x , and I_{∞} stand for fluorescence intensities of HN12 in the absence, at an intermediate concentration of lipid and at saturation level of interaction, respectively. Figure 3 reveals a linear regression for the plot of $(I_{\infty} - I_0)/(I_x - I_0)$ versus $[\text{lipid}]^{-1}$ and yields a value of partition coefficient, $K_p = (5.99 \pm 1) \times 10^4$ in DMPC and $K_p = (2.32 \pm 1) \times 10^5$ in DMPG. Such high magnitudes of K_p are, indeed, a clear manifestation of efficient partitioning of the probe in liposome membranes. Apart from being consensus with literature reports,^{1,7–11,36} the K_p values indicate greater partitioning of the probe in anionic DMPG membrane compared to that in zwitterionic DMPC membrane.

Experimentally calculated values of partition coefficient are further reinforced from results of docking studies in the forthcoming section. A lower magnitude of inhibition constant for binding interaction of HN12 with DMPG lipid-bilayer compared to that with DMPC (516.01 μM in DMPG vs 722.83 μM in DMPC; section 3.7) substantiates the higher K_p with DMPG lipid (Table 1).

3.3. Steady-State Fluorescence Anisotropy Study. Measurement of fluorescence anisotropy (r) is important because it provides fruitful information about the physical characteristics and the nature of the environments around the fluorophore.^{7,11,12,20a,21,25,29} Modulation in fluorescence anisotropy with varying lipid concentration will reflect the degree of rigidity imposed on the probe by the microheterogeneous media.^{11,37} As depicted in Figure 4, an increase in anisotropy of HN12 with increasing concentration of lipid indicates that the fluorophore experiences a motionally confined environment inside the lipids. Attainment of a plateau region in Figure 4 implies saturation in the interaction between the two parties. A considerably high value of anisotropy of HN12 at the saturation level of interaction indicates that the probe experiences a substantially rigid environment inside the DMPC and DMPG membranes.

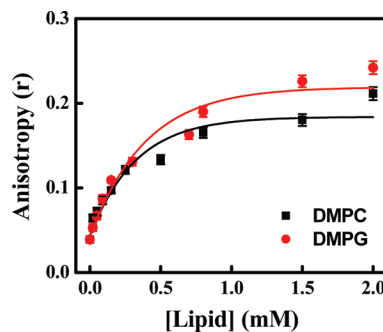


Figure 4. Variation of steady-state fluorescence anisotropy (r) as a function of lipid concentration ($\lambda_{\text{ex}} = 300 \text{ nm}$ and $\lambda_{\text{monitored}} = \lambda_{\text{em}}^{\max}$). The points denote the actual values and the solid line denotes the best sigmoidal fit to the data. Error bars are within the symbols if not apparent (each data point is an average of ten individual measurements).

Thus, the steady-state fluorescence anisotropy measurements seem to strongly complement the steady-state emission spectral observations. An increase in the anisotropy value of HN12 in DMPG lipid environment is relatively greater than that in DMPC lipid at the same concentration of the probe and the lipid (Figure 4). This finding is a nice corroboration to the stronger binding interaction of the probe with DMPG as compared to DMPC lipid and is consistent with the results discussed in the previous section (section 3.2).^{7,11,12,29}

3.4. Wavelength Sensitive Fluorescence Parameter: The Red-Edge Excitation. Red edge excitation shift (REES)⁴⁰ is a well-known phenomenon that provides a more vivid picture of the surrounding atmosphere of the probe while emitting from an excited state, particularly when being in an organized medium. REES measurement is exploited extensively in biochemical and biophysical research^{12,20,41,42} for its excellent ability to furnish important information regarding direct monitoring of solvation dynamics within organized media.^{41,42} REES is the phenomenon of shifting of the emission maxima to the red upon shifting the excitation wavelength to the red end of the absorption spectrum. Precisely, the operation of REES is subject to the following conditions:^{11,41} (a) The molecule should be polar with dipole moment higher in the excited state than that in the ground state. In fact, the extent of inhomogeneous broadening of the absorption spectra allowing the provision of site photo-selection of energetically different species is dependent on the change of dipole moment ($\Delta\mu$) upon photoexcitation through the relation $\Delta\nu = A\Delta\mu\rho^{-3/2}(kT)^{1/2}$ according to Onsager sphere approximation^{41a} (here A is a constant that depends on the dielectric constant of the medium and ρ is the Onsager cavity radius). However, additional broadening, which can play even a greater role in inhomogeneous broadening of absorption spectra, may be induced by specific interactions of the sort of hydrogen bonding, electrostatic interactions and so forth.⁴¹ (b)

TABLE 1: Relevant Parameters for Binding of HN12 with Lipids

sample	partition coefficient, K_p	binding energy ^a	inhibition coefficient ^a	K_{SV}^b	intercept of SV plot ^c	R^d
HN12					8.31	0.98
HN12 in DMPC	$(5.99 \pm 1) \times 10^4$	-4.29	722.83	4.56	1.05	0.99
HN12 in DMPG	$(2.32 \pm 1) \times 10^5$	-4.48	516.01	16.45	0.98	0.99

^a Binding energy (in kcal/mol) and inhibition coefficient (in μM) are derived from docking studies. ^b K_{SV} (M^{-1}) is the Stern–Volmer quenching constant for quenching of bare (in aqueous buffer) and lipid-bound HN12 ($[\text{lipid}] = 1.0 \text{ mM}$) by transition metal ion quencher, Cu^{2+} .

^c Ideally the intercept of Stern–Volmer (SV) plot should be equal to 1. Here, the value of the intercept justifies the excellence of the linear regression according to Stern–Volmer relation, i.e., an estimate of deviation from the ideal case. ^d R is the correlation coefficient to justify the excellence of the linear fit to the actual data points. The fitting operation is performed with the algorithm implemented in MS Origin 6.1.

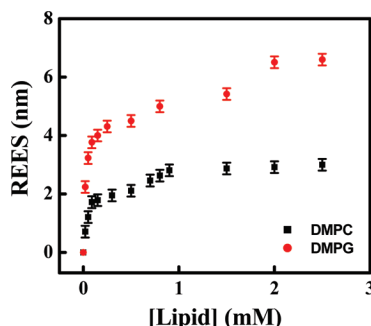


Figure 5. Plot of REES ($\Delta\lambda_{\text{em}}^{\max}$ in nm) against lipid concentration (in mM). Error bars are within the symbols if not apparent (each data point is an average of four individual measurements).

The solvent molecules around the fluorophore must be polar and the solvent reorientation time ($\langle\tau_{\text{solvent}}\rangle$) should be slower or comparable to the fluorescence lifetime (τ_f) of the fluorophore so that unrelaxed fluorescence can give rise to excitation-wavelength-dependent emission behavior.

It is seen that the probe molecule HN12 exhibits a shift of the emission maxima toward the red with shifting of the excitation wavelength to the red end of absorption spectra (during REES measurements meticulous care has been devoted to the selection of excitation wavelength to ensure that the variation of λ_{ex} involves shift to the red end of the absorption spectra and not merely the absorption maxima. This is very crucial in REES experiments⁴¹). Figure 5 displays that increase in lipid concentration associates increase in magnitude of REES for the same change of excitation wavelength and under same experimental conditions.

Now, because the lifetime measurements confirm that binding of HN12 with lipid-bilayer accompanies an increase of fluorescence lifetime compared to that in pure aqueous buffer (Table 2) and the mean (average) lifetime values are quite high, it seems reasonable to state that the observed REES in the studied organized media is not due to fluorescence from an unsolvated (or partially solvated and, hence, incompletely relaxed) state, rather fluorescence occurs from fully solvated state in these systems since the fluorescence lifetimes might be longer than (or comparable to) the solvent relaxation time. Rather some other sort of interactions seems to play the governing role in creating a distribution of energetically different molecules in the ground state that allows their photoselection. This idea goes in line with other studied systems for REES in different environments.^{11,29,41,42} From the structural point of view, the unique nature of HN12 is quite interesting in the sense that it contains two functional groups capable of forming hydrogen bond, but the $-\text{OH}$ group can enter into hydrogen bonding primarily by donating the hydrogen atom whereas the $-\text{CHO}$ moiety by acting as hydrogen acceptor. That hydrogen bonding interactions in different environments leads to further complicity in the

photophysics of HN12 is evident from its photophysical studies.³⁰ Thus, it seems reasonable that different types of hydrogen bonding interaction and their perturbations or modifications to different extents in different complex environments provided by the microheterogeneous environments of the lipids might play the crucial role in producing ground state inhomogeneity and thereby allowing initial photoselection. This conjecture receives further credence with a view to the fact that the extrinsic probe HN12 is located in the headgroup region of the lipid-bilayers (as has been argued in forthcoming section). However, to be very particular about the reason stated above is not quite easy given the inherently complex nature of hydrogen bonding interaction and also the complexity provided by the microheterogeneous environments of the lipids.

3.5. Effect of Phase Transition in Lipid on the ESIPT

Emission of Lipid-Bound Probe. The study of phase transitions of phospholipids has long been an active topic of research,¹⁰ and the well studied phospholipids in this respect are DMPC, DMPG, and DPPC, which are characterized by a transition temperature (T_m) of approximately 23 °C (for DMPC and DMPG) and 42 °C (for DPPC). The endothermic reaction observed by differential scanning calorimetry⁴³ at this temperature (T_m) marks the onset of liquidity of the hydrocarbon region of the lamellar phase.²⁵ The loss of crystallinity has been characterized by an X-ray diffraction study.⁴⁴ A survey of the literature reveals the remarkable modifications of the properties of lipid membrane associated with this transition and the techniques used to detect them, such as a decrease in the thickness of the lipid membranes,⁴⁴ a change in the bilayer volume as detected by dilatometry,⁴⁵ a marked decrease in the ¹H NMR line width,⁴⁶ a decrease in the order parameter of the ESR probes,⁴⁷ and decrement of fluorescence anisotropy/polarization of various probes.^{9–11,36}

It is reported that, above the characteristic phase transition temperature (T_m), the amphiphiles diffuse freely and the membrane behaves like a two-dimensional fluid, while below T_m , this diffusion is slowed down.¹ That the solid to liquid crystalline phase transition exerts remarkable effects on the permeability of phospholipid membranes¹⁰ afforded us the impetus for investigating the influence of this phase transition on the emission characteristics of lipid-bound HN12. Figure 6a reveals a simple execution of the effort by observing only the change of tautomer (PT) emission intensity ($\lambda_{\text{em}} = 480$ nm) as a function of temperature at a particular DMPC/DMPG concentration (1.0 mM). The ESIPT emission of HN12 is found to exhibit specific variation with temperature through the appearance of a sigmoidal curve whose midpoint corresponding to T_m stands in the range 22.0–25.0 °C, that is, a value in excellent consensus with available literature data for T_m of the studied lipids.^{1,10,11,36,39} Repetition of the same experiment with other concentrations of lipid also ([lipid] = 0.75 and 2.0 mM) yielded the same reliable result. Figure 6b illustrates representative

TABLE 2: Time-Resolved Fluorescence Decay Parameters, Quantum Efficiency, and Radiative and Nonradiative Decay Rate Constants of HN12 in Lipids

HN12 in ↓	$\tau_1/\text{ns} (\alpha_1)$	$\tau_2/\text{ns} (\alpha_2)$	$\tau_3/\text{ns} (\alpha_3)$	$\langle\tau_f\rangle/\text{ns}$	χ^2	Φ_f	$k_r^a (\text{s}^{-1})$	$k_{nr}^b (\text{s}^{-1})$
aqueous buffer	0.087 (0.91)	0.588 (0.09)		0.287	1.50	0.007	2.433	3.459
0.5 mM DMPC	0.701 (0.031)	3.228 (0.001)	0.062 (0.967)	0.348	1.19	0.011	3.161	2.842
1.0 mM DMPC	0.517 (0.035)	2.021 (0.0363)	0.544 (0.929)	1.131	1.02	0.022	1.945	0.865
1.5 mM DMPC	0.531 (0.039)	1.975 (0.042)	0.0509 (0.92)	1.174	1.13	0.033	2.811	0.824
0.5 mM DMPG	0.731 (0.024)	2.961 (0.0099)	0.0543 (0.966)	1.031	1.09	0.012	1.164	0.958
1.0 mM DMPG	1.362 (0.053)	3.928 (0.0086)	0.055 (0.783)	1.562	1.19	0.034	2.177	0.618
1.5 mM DMPG	1.573 (0.079)	6.237 (0.0045)	0.052 (0.917)	2.074	1.19	0.056	2.7	0.455

^a k_r values are $\times 10^{-7}$ order. ^b k_{nr} values are $\times 10^{-9}$ order.

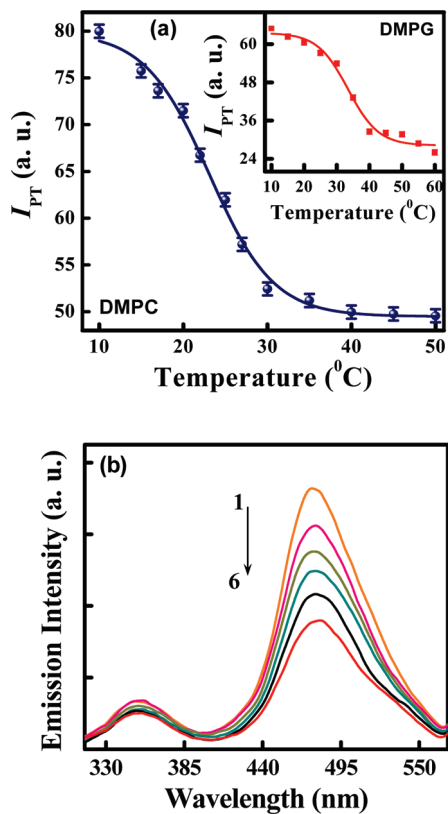


Figure 6. (a) Plot of variation of intensity of proton transferred emission ($I_{PT} = I_{480 \text{ nm}}$) of HN12 as a function temperature at a particular concentration of lipid ($[\text{DMPC}] = 1.0 \text{ mM}$ and $[\text{DMPG}] = 1.0 \text{ mM}$ in inset). The points denote the actual values and the solid line denotes the best sigmoidal fit to the data. The midpoint of the transition curves corroborates to the phase-transition temperature (T_m) of the lipids. Error bars are within the symbols if not apparent. (b) Temperature-induced modulations on the emission profile of lipid-bound HN12. Representative spectra are given for HN12 in 1.0 mM DMPG with curves 1–6 corresponding to $t = 10, 20, 30, 40, 50$, and 60°C .

spectra showing the modulations on emission profile of DMPG-bound HN12 with increasing temperature. Similar behavior has been reported for other probes like 1-naphthol and 3-hydroxyflavone.¹⁰

It appears imperative to note at this stage that the temperature dependence of HN12 emission properties in bulk homogeneous fluid registers a noticeable difference from those in lipid environments. In bulk homogeneous solvent, rise of temperature accompanies decrease of HN12 tautomer (PT) emission at $\lambda_{em} \approx 480 \text{ nm}$ with concomitant enhancement of the open conformer emission at $\lambda_{em} \approx 353 \text{ nm}$. This effect has been elaborately discussed in a previous report³⁰ and is also mentioned in the Supporting Information (Figure S2). The reduction of HN12 tautomer emission with rising temperature is argued on the basis of enhanced nonradiative decay rate constant (k_{nr}), while for the open conformer, an increase in k_{nr} is likely to be dominated by an increase in population showing an overall increase in intensity. Conversely, for lipid-bound HN12, both the open conformer and tautomer counterparts are seen to experience depletion of emission intensity with increasing temperature. However, the variation of PT emission exhibits a specific pattern as a function of temperature, marking an indication toward its sensitivity for the phase change in the membrane (Figure 6a); the effect of temperature on the open conformer emission is rather gradual and less sensitive to the phase change (Figure S3 of Supporting Information).¹⁰ While in homogeneous solvent, for neither PT nor the open conformer emission band, any

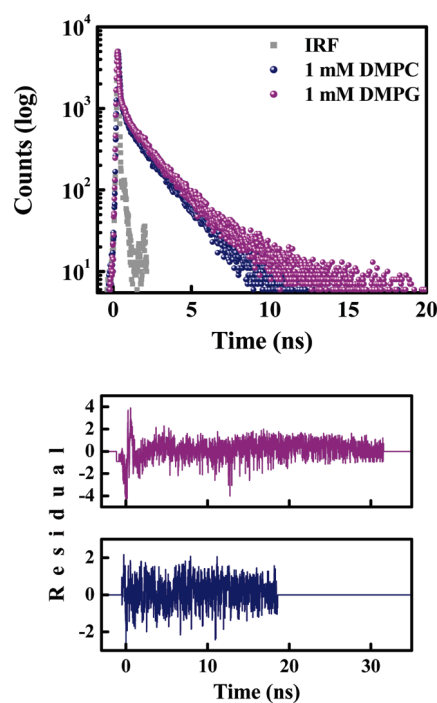


Figure 7. Typical time-resolved fluorescence decay profile of lipid-bound HN12 ($\lambda_{ex} = 375 \text{ nm}$ and $\lambda_{monitored} = \lambda_{em}^{\max}$). Representative decay patterns for HN12 in 1.0 mM DMPC and 1.0 mM DMPG are given. The lower panel shows the plot of residual for the respective fitted functions to the actual data.

specific variation with temperature similar to that illustrated in Figure 6a is noted (Figure S2 of Supporting Information and ref 30).

3.6. Time-Resolved Measurements. (a) Time-Resolved Fluorescence Decay. By virtue of its sensitivity to the environments and excited state interactions, fluorescence lifetime serves as an indicator to explore the environment around a fluorophore.^{7,8,11,48} It also furnishes valuable information regarding binding of a probe with vesicles.^{7,11,20,21,26,29,42} Here, we have monitored the fluorescence lifetimes of HN12 in the presence of increasing lipid concentration. Figure 7 illustrates the typical time-resolved fluorescence decay profiles of the probe in various environments indicated in the figure legends and the corresponding fitting parameters are collected in Table 2. In view of the complicated functional and structural architecture of liposome membranes, it is not surprising to have a multieponential decay profile of HN12 in the presence of DMPC and DMPG lipids; indeed, the decay of HN12 in pure aqueous buffer also follows a biexponential pattern.³⁰ Thus, in spite of placing too much emphasis on the individual decay time constants, it is rational to employ the mean (average) fluorescence lifetime as an important tool to decipher the behavior of HN12 when present in the microheterogeneous environments of the lipids.^{7,11,20,21,26,29,42,49}

In analogy to literature reports^{7,11,20,21,26,29,42,49} and modulations of excited state photophysics of the probe in constrained environments of proteins, micelles, and cyclodextrins,²⁹ the increase of lifetime associated with increasing lipid concentration (Table 2) seems attributable to diminution of nonradiative decay channels through reduction of rotational/vibrational degrees of freedom resulting from its encapsulated state in the lipid environments. To further construe the modulations in excited state behavior of HN12, we have calculated the radiative (k_r) and nonradiative (k_{nr}) decay rate constants (Table 2) using the following two equations:^{11,29}

$$k_r = \frac{\Phi_f}{\langle \tau_f \rangle} \quad (8)$$

$$k_{nr} = \frac{1}{\langle \tau_f \rangle} - k_r \quad (9)$$

Here, Φ_f is the fluorescence quantum efficiency and $\langle \tau_f \rangle$ is the average fluorescence lifetime calculated from eq 3. Scrutiny of the data in Table 2 distinctly reveals that the radiationless decay rates are considerably reduced in lipid environments compared to that in bulk aqueous buffer medium, whereby substantiating our previous assignments.

(b) Time-Resolved Fluorescence Anisotropy Decay. To obtain further insight into the microenvironment around the probe, a time-resolved fluorescence anisotropy decay study of HN12 in aqueous buffer and in the lipid environments has been performed. The time-dependent decay of fluorescence anisotropy is a sensitive tool for gathering information about the rotational motion and rotational relaxation of the fluorophore in an organized assembly.^{7,11,31a,50,51} The typical anisotropy decay profile of HN12 in aqueous buffer as well as lipid environments is presented in Figure 8. It is, indeed, surprising to note that the probe exhibited an unusual “dip-and-rise” pattern in the fluorescence anisotropy decay in aqueous buffer solution with the prominence of the specific dip-and-rise pattern being progressively obscured with increasing lipid concentration. Such dip-and-rise kind of profile is a signature for the juxtaposition of at least two populations, one with a short fluorescence lifetime and a short rotational correlation time and another having both the time constants longer compared to those of the first population.^{11,31a,50} This sort of anisotropy decay behavior has been described as associated anisotropy by Lakowicz¹¹ and has been previously observed in several situations.^{11,31a,50} However, usually this kind of anisotropy decay profile has been observed for fluorophores in confined environments in which the faster motion is attributed to the solvent exposed groups/moieties of the fluorophore and the slower motion to the bound counterpart, with the usual trend that the appearance of the “dip-and-rise” pattern is rendered more prominent with increasing degree of confinement.^{11,31a,50} It was initially quite puzzling for us to note a qualitatively reverse trend (with respect to usual reports found in the literature^{11,31a,50}) in the present findings in the form that the dip-and-rise pattern is more prominently seen for HN12 in bulk aqueous buffer phase, while it is gradually obscured with increasing lipid concentration. Hence, it was the very first requirement of the state of affairs to establish the reproducibility of the findings, which has been confirmed by performing the experiments repeatedly, maintaining the same experimental conditions and instrumental settings.

Now, as we endeavor to rationalize the origin of the present findings, we found that this kind of a bit unusual time-resolved anisotropy decay behavior has been interpreted according to an associated exponential model in which the fluorescence lifetime and amplitude of the total intensity decay components are linked specifically with individual anisotropy parameters.^{50a,g,h,52}

$$r(t) = \sum_{i=1}^n f_i(t) r_i(t) \quad (10)$$

$$f_i(t) = \frac{\alpha_i \exp(-t/\tau_i)}{I_T(t)} \quad (11)$$

$$I_T(t) = \sum_{i=1}^n \alpha_i \exp(-t/\tau_i) \quad (12)$$

$$r_i(t) = (r_{0,i} - r_{\infty,i}) \exp(-t/\theta_i) + r_{\infty,i} \quad (13)$$

in which θ_i is the i^{th} rotational correlation time, α_i and τ_i are the i^{th} fluorescence amplitude and lifetime, respectively, and $r_{0,i}$ is the initial prerotational anisotropy.^{50g,52} The nomenclature is kept same as those described elsewhere.⁵² Several attempts in the literature have rightly emphasized on the time-dependent weighting factor, $f_i(t)$, in accounting for the dip-and-rise nature in the anisotropy decay profile,^{11,31,50} and it is argued that this type of anisotropy decay profile is best obtained when the two lifetime values are significantly different.^{11,31,50} This prerequisite is evidently satisfied for HN12 in aqueous buffer phase, as can be seen in Table 2. The time-resolved fluorescence decay behavior of HN12 (i.e., lifetime measurement) in aqueous buffer phase (Tris-HCl buffer, pH 7.4) does not significantly deviate from that in pure aqueous solution. In bulk aqueous buffer phase the time-resolved fluorescence decay behavior of HN12 reveals the presence of a fast decaying major ($\sim 91\%$) component and a slow minor component.³⁰ The major component is attributed to the proton-transferred (PT) form of HN12 (Conformer-T in Scheme 1 (the proton-transferred form is obviously the mostly populated conformer upon the excited surface³⁰)) while the minor component corresponds to the fluorescence lifetime of the open solvated (hydrated) form of HN12. In fact, the spectral signature for the presence of the solvated structure of HN12 has been obtained and confirmed from the absorption spectral characteristics of HN12 in aqueous and other aprotic media, like acetonitrile, and are reported elsewhere.³⁰ This finding has been ascribed to intermolecular hydrogen bonding-assisted nonradiative decay channels operating in protic media and is more elaborately discussed in the previous report.³⁰ Thus, with a view to such photophysical characteristics of the probe molecule (HN12), it appears evident that encapsulation of HN12 within the confined environments provided by the liposome systems should accompany a reduction in the degree of solvent-induced perturbation to the ESIPT of HN12. This postulation is, in fact, found to be quite well supported by the time-resolved fluorescence decay behavior of HN12 in the liposomes, as illustrated in Table 2. These findings are also found to be in consensus with the behavior of the probe in other constrained environments provided by proteins²⁰ and other supramolecular assemblies like cyclodextrins and micelles.²⁹ Therefore, it is not unlikely to obtain such modulation of photophysics of the probe molecule within the studied liposome systems.

Now, at this stage, it is not unlikely if we consider the origin of the dip-and-rise pattern of fluorescence anisotropy decay of HN12 in the aqueous buffer phase to be emanating from contributions from the PT form of HN12 and the solvated structure. This is obvious that the population of the solvated structure of HN12 will be progressively discouraged with increasing lipid concentration, whereby resulting in obscuring the appearance of the dip-and-rise pattern in the anisotropy decay profiles (Figure 8). Clearly, interplay between different intramolecular and intermolecular motions is being invoked here to account for the observed anisotropy decay profile. Therefore, modulations of these motions upon interaction with the liposome

where

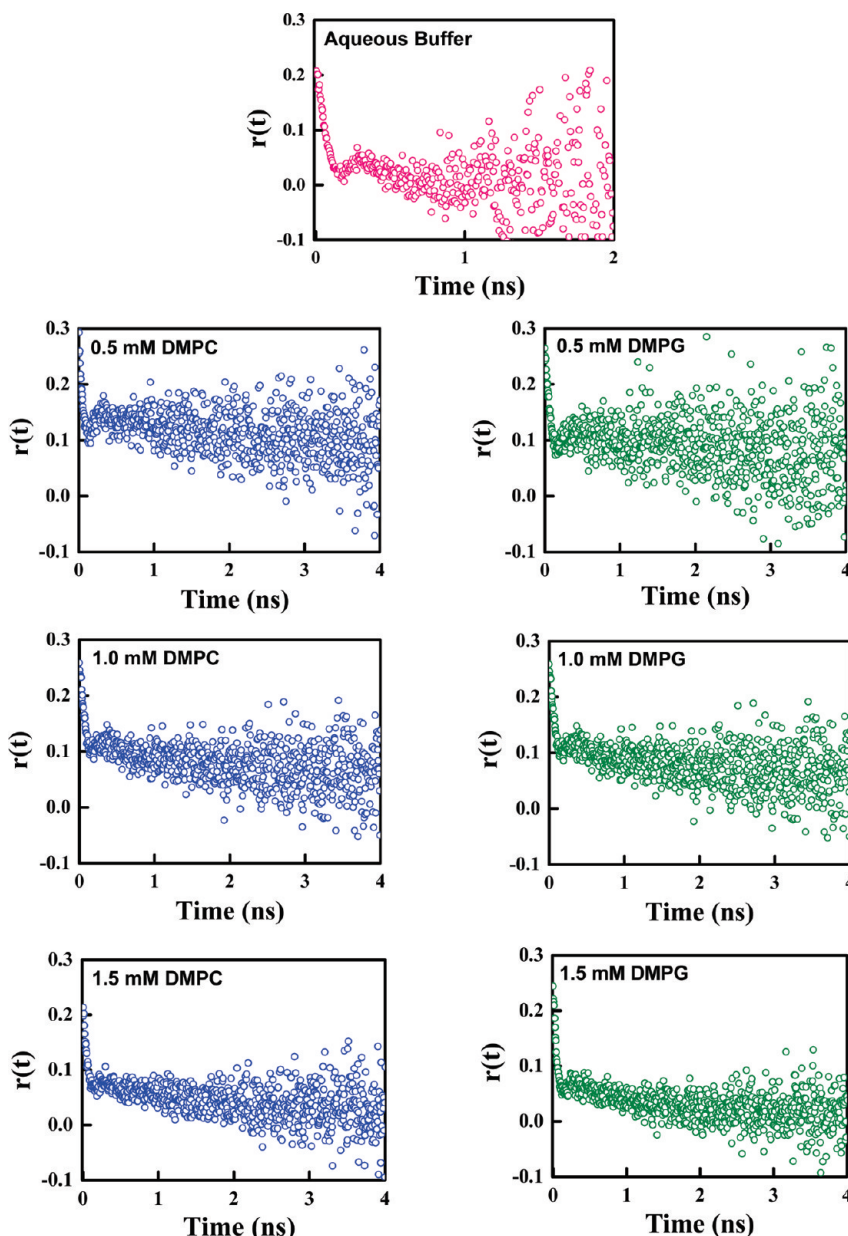


Figure 8. Time-resolved anisotropy decay profile of HN12 in various environments, as indicated in the figure legend ($\lambda_{\text{ex}} = 375 \text{ nm}$ and $\lambda_{\text{monitored}} = \lambda_{\text{em}}^{\max}$).

membranes should naturally contribute to governing the overall motional dynamics of the probe within the lipid environments. However, with a view to the observation of enhancement of the average fluorescence lifetime of HN12 upon binding to the lipids and the possibility of coupling of the motions of the probe with global tumbling motion of the liposome units, the internal motions of the probe can not be considered as the sole criterion for generating the dip-and-rise anisotropy profile.^{50a}

One major utility of time-resolved anisotropy decay measurements often convoys its applicability in deciphering the important aspect of evaluation of the binding site of the probe through calculation of the generalized order parameter (S) in the course of monitoring the rotational relaxation dynamics of a fluorophore in an organized medium.⁵¹ This was, indeed, one of the initial objectives of the measurement in our case. For this purpose, we fitted the anisotropy decay curves for HN12 in the presence of a substantial lipid concentration ([lipid] = 1.5 mM) with two rotations only (one fast and another slower rotation).^{50c} The fitted parameters are as follows: for HN12 in 1.5 mM DMPC, the

two rotational relaxation times are $\theta_1 = 34 \text{ ps}$ ($\alpha_{1r} = 0.74$) and $\theta_2 = 1.62 \text{ ns}$ ($\alpha_{2r} = 0.26$) with $\chi^2 = 1.21$, and for HN12 in 1.5 mM DMPG, the values are $\theta_1 = 33 \text{ ps}$ ($\alpha_{1r} = 0.75$) and $\theta_2 = 1.25 \text{ ns}$ ($\alpha_{2r} = 0.25$) with $\chi^2 = 1.25$.

The order parameter (S), as defined as $S^2 = \alpha_{2r}$,^{11,51} provides information about the motional restrictions on the probe molecule. It is a measure of the spatial restriction having values ranging from 0 (corresponding to unrestricted motion) to 1 (for complete restriction on the motion).^{11,51} The calculated values for the order parameter are $S = 0.51$ in DMPC and 0.50 in DMPG lipid. Such a reasonably high magnitude of the order parameter suggests the binding site of the probe to be in the lipid headgroup region (section 3.7)⁵¹ and are found to be consistent with literature reports.^{51a,b} From NMR relaxation data^{51e,f} and other experimental techniques^{50–52} it has been documented that there is a higher degree of order near the surface than in the interior of liposome systems. In fact, in the hydrocarbon interior of the liposomes the order parameter is

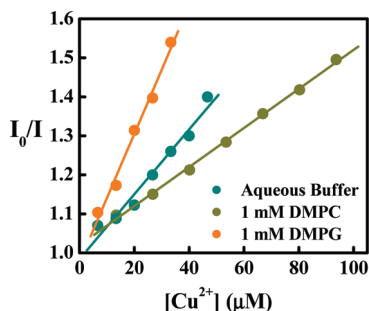


Figure 9. Stern–Volmer plot for Cu²⁺-ion-induced fluorescence quenching of HN12 in aqueous buffer medium and in the presence of the lipids ([DMPC] = 1.0 mM, [DMPG] = 1.0 mM). The respective environments are specified in the figure legend.

known to be enormously low, because the wobbling motion of the probe is expected to be almost isotropic.^{51e–h}

3.7. Location of the Probe. The foregoing discussions clearly establish the occurrence of interaction of the ESIPT probe HN12 with DMPC and DMPG lipids. The present section is thus designed to explore the very pertinent as well as important issue of assessing the location of the probe in the lipid environments. It is, indeed, quite difficult to deduce an idea about the precise location of the extrinsic molecular probe. Nevertheless, insertion of external perturbations to the photophysics of lipid-bound HN12 and a careful monitoring of its response emerged to form the basis for assessing the location of HN12 in the studied lipids.

(a) **Fluorescence Quenching Experiments.** In an attempt to externally modify the photophysics of lipid-bound HN12 we adopted the strategy of quenching of fluorescence intensity by a heavy metal ion quencher, Cu²⁺. The transition metal cation Cu²⁺ is well-known for its quenching action and is seen to quench the fluorescence of bare HN12 (HN12 in Tris-buffer) as displayed in Figure 9. Quite interestingly the extent of quenching is observed to be appreciably enhanced when HN12 is present in DMPG lipid while in DMPC lipid the extent of quenching is seen to be the minimum. This result receives a sound interpretation following the postulation of location of the probe in lipid headgroup region. Favorable electrostatic affair (attractive) between the negatively charged DMPG headgroup and positively charged quencher (Cu²⁺) should ascertain a closer approach of the quencher to the fluorophore subsequently leading to an increased degree of quenching. An added impact of this sort should be absent in case of HN12 in buffer. Whereas, for HN12 in DMPC lipid having zwitterionic character, the cationic quencher, Cu²⁺ ion, fails to encounter an appreciable interaction. Such modulations in extent of fluorescence quenching of HN12 depending on its surrounding atmosphere could not be expected for its penetration into the hydrocarbon interior of lipid-bilayers as the hydrophobic environment of the region must have restricted incursion of the ionic quencher, Cu²⁺.^{1,5,7,45,49} A quantitative estimate of the quenching results is presented in Table 1 in terms of Stern–Volmer constant (K_{SV}) as derived from the Stern–Volmer relation:¹¹

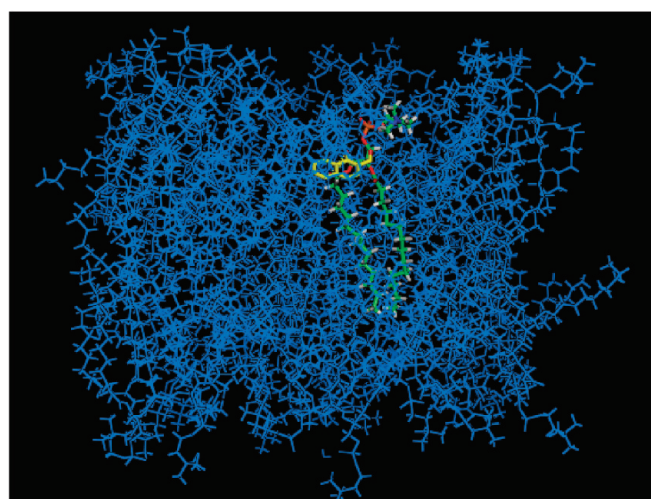
$$\frac{I_0}{I} - 1 = K_{SV}[\text{quencher}] \quad (14)$$

Here, I_0 and I are, respectively, the fluorescence intensities in the absence and presence of the quencher, Cu²⁺, and the term within square bracket represents respective concentration.

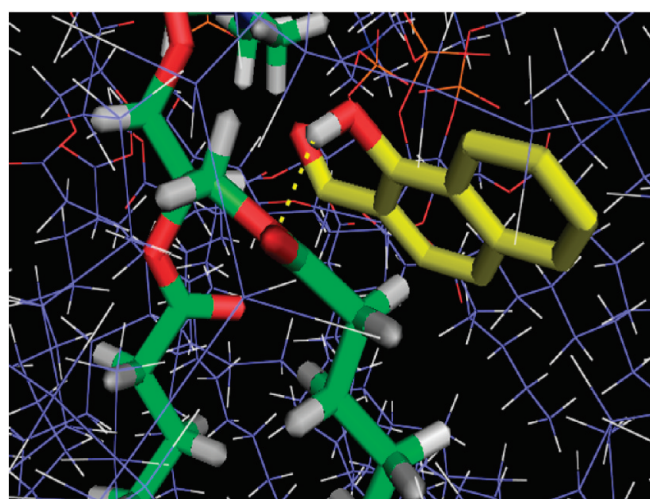
Now, as we endeavor to frame an interpretation for the observed emission intensity enhancement of HN12 upon interaction with the studied lipids and find a reasonable consistency between our steady state and time-resolved data, it could be imperative to focus on hydrogen bonding property of HN12, which could also be helpful in assessing molecular interaction mechanism between the molecular probe and the lipids.⁵³ Some recent investigations by Zhao et al. have explored the crucial influence that intra- and intermolecular hydrogen bonding interactions can exert on fluorescence properties of a fluorophore.^{53a,54} Both the intermolecular (I_{er}MHB) and intramolecular (I_{ra}MHB) hydrogen bonding can act as effective conduit to facilitate nonradiative deactivation of excited fluorophores.⁵⁴ In some recent reports, Zhao et al. have argued that a comparatively stronger I_{ra}MHB tends to assist an enhanced rate for intersystem crossing (ISC),^{53–55} while I_{er}MHB can facilitate internal conversion (IC).^{53–55} Thus, it appears logical to think that both the modes of nonradiative deactivation will be operative for HN12 in aqueous buffer. The impact of solute–solvent I_{er}MHB interactions on the photophysics of HN12 in protic media has been observed and discussed in a previous report³⁰ and is also reflected on the modulations of the time-resolved fluorescence decay behavior of HN12 upon interaction with the lipids (section 3.6).²⁹ It is, thus, obvious that partitioning of the probe from the aqueous phase to the constrained lipid environments would discourage the solute (HN12)–solvent (water) I_{er}MHB,³⁰ whereby tending to reduce the nonradiative deactivation via an IC process. However, it is ethical to point out at this stage that a precise description of relative contributions of each component of the deactivation processes is quite difficult given the complex microheterogeneous environment provided by the lipids. The I_{er}MHB interactions of HN12 with the functional moieties in the lipid headgroup region (as discussed in sections 3.4 and 3.7) should still make IC possible and the I_{ra}MHB in HN12 should still promote the ISC. Thus, the observed overall modulation of photophysics of HN12 within lipid environments should be treated as the net resultant effect of several complex effects like varied polarity of immediate vicinity of probe molecules,^{6,7,11,20,29,42,49} modification of radiative and nonradiative decay channels, and so forth. The net resultant appears to describe the fluorescence enhancement of HN12 in lipids in terms of reduction of nonradiative decay rate constant (k_{nr}) with increasing lipid concentration (vide section 3.6, Table 2). Indeed, because the environments surrounding the probe molecules in homogeneous (bulk aqueous) and heterogeneous (lipid) phases are enormously different, we do not find it encouraging to compare the two environments directly.

In this connection, it appears pertinent to figure out that the role of photoinduced electron transfer (ET) from protic solvents to the chromophore assisted by hydrogen bonding might put its signature in the process of fluorescence quenching and hence the overall photophysics occurring within the system in hydrogen-bonding environment. Zhao et al.^{54a} in a recent nice report have explored the phenomenon on oxazine 750 (OX 750) chromophore and have described it as a new fluorescence quenching mechanism for chromophores in protic solvents operating via site-specific I_{er}MHB interactions and have explored the effect through femtosecond time-resolved stimulated emission pumping fluorescence depletion spectroscopy combined with high level theoretical calculations. With HN12 also we notice a relative decrement of fluorescence quantum yield of HN12 on passing from aprotic to protic solvents³⁰ and qualitatively assign the effect on the operation of solute–solvent I_{er}MHB-assisted radiationless deactivation channels.⁵⁴ A direct comparison of

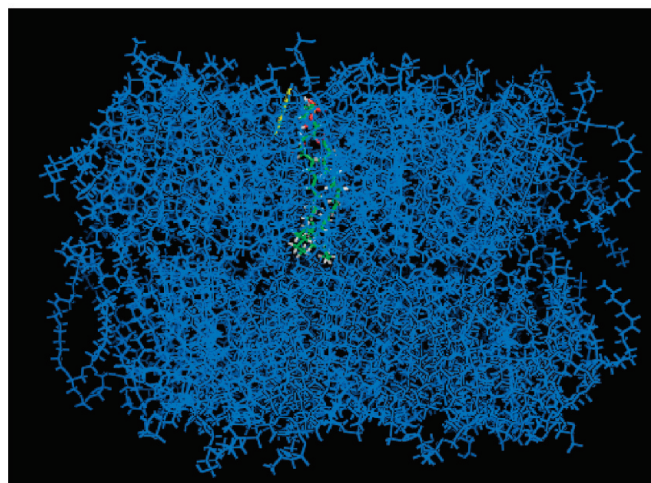
(a)



(b)



(c)



(d)

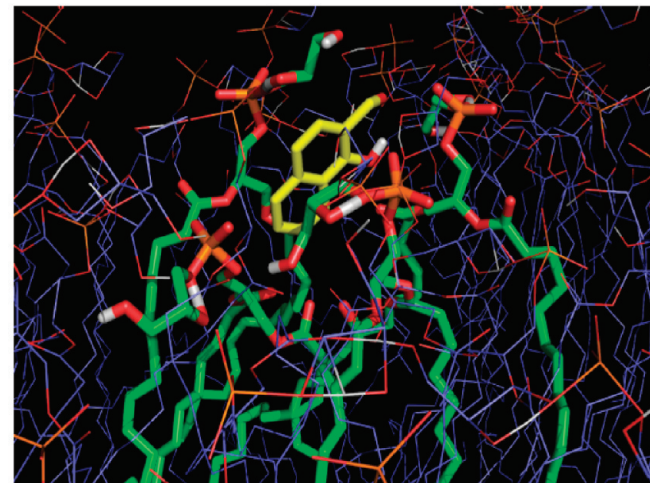


Figure 10. Stereoview of the docked poses of HN12 with the lipids: (a) docked pose of HN12 with DMPC lipid-bilayer, (b) magnified view of the site of interaction of HN12 with DMPC, (c) docked pose of HN12 with DMPG lipid-bilayer, and (d) magnified view of the site of interaction of HN12 with DMPG.

our results with the report of Zhao et al. reveals that the observed fluorescence quenching of HN12 with increasing hydrogen bond forming ability of the protic solvents is not as drastic in magnitude as in case of OX 750. Thus we presume that the action of protic solvents resulting in quenching of fluorescence quantum yield of HN12 in our case is primarily based on solute–solvent I_eMHB-assisted activation of nonradiative decay routes,⁵⁴ and specific interaction of the sort of protic solvent-to-chromophore ET reaction might not be playing an instrumental role here, as in that case a considerably more drastic quenching effect would have been observed.

(b) **Docking Studies.** The foregoing discussions regarding the probable location of the extrinsic probe HN12 in complex lipid environments is substantiated with a reinforcing support from docking measurements. Docking studies unveil that the preferred conformation of HN12 with favorable binding interaction is achieved when HN12 is located in the headgroup region of the lipid-bilayers as illustrated in Figure 10. As displayed in Table 1, negative binding energy of HN12 with both the lipids dictates a favorable binding interaction, while the inhibition constant values seem to support the observation of a higher partition coefficient of HN12 in DMPG lipid compared to DMPC (section 3.2).

Also, the location of the probe in the polar headgroup region of both lipids (as displayed in the docked pose in Figure 10) seems to ascertain the possibility of hydrogen bonding interactions of HN12 with the functional moieties present in the headgroups of the lipids (Scheme 1), whereby corroborating the role of specific interactions (of the sort of hydrogen bonding, electrostatic interactions, etc.) in creating inhomogeneous broadening of the absorption spectra, which subsequently allows the provision of site photoselection as observed in the course of REES experiments discussed in section 3.4.

4. Conclusion

The present investigation demonstrates the modulations of photophysics of a potent ESIPT molecule, namely, HN12 upon interaction with supramolecular assemblies of an anionic and a zwitterionic liposome membrane. In particular, the remarkable modifications of the emission profile of HN12 upon binding to the lipids dictate the sensitivity of its excited-state photophysics toward the interaction, with special emphasis being delivered to ESIPT reaction. Quantitative analysis of the emission data advocates for a greater degree of partitioning of the extrinsic probe into DMPG lipid than DMPC. Other experimental findings

(like steady-state anisotropy, REES, time-resolved measurements, and so forth) are found to substantiate these results. Ionic quencher (Cu^{2+})-induced fluorescence quenching and docking studies indicate the location of the probe to be in the headgroup region of the lipids. The tautomer emission of the extrinsic probe HN12 is also found to exhibit specific variation in response to phase transition in the lipids. It is well-known that the lipid phase transition and membrane fluidity parameters owe huge significance to biological functioning of the membrane. Hence, the study of physical properties of these membranes is of paramount importance. The present work demonstrates an effort to decipher the microheterogeneous environments of lipids by monitoring the modified photophysics of the external probe upon interaction with the studied lipids.

Acknowledgment. B.K.P. acknowledges C.S.I.R., India, for the research fellowship. N.G. acknowledges C.S.I.R. (Project No. 01(2161)07/EMR-II) and DST (Project No. SR/S1/PC/26/2008), Government of India, for financial support. The authors gratefully acknowledge the instrumental facility of Indian Association for the Cultivation of Science, Jadavpur, Calcutta, India, for time-resolved measurements. We appreciate the cooperation received from Dr. K. P. Das, Mr. V. Banerjee, and Mr. P. Dey of Bose Institute, Calcutta, India, for DLS measurements. We convey our special thanks to Dr. Nitin Chattopadhyay, Chemistry Department, Jadavpur University, India, for his valuable discussions. The authors greatly appreciate the constructive suggestions from the reviewers.

Supporting Information Available: Information on the dynamic light scattering (DLS) measurement and the effect of temperature on the ESIPT emission of HN12 in bulk homogeneous solvent and on the emission of the open conformer of lipid-bound HN12. This material is available free of charge via the Internet at <http://pubs.acs.org>.

References and Notes

- (1) (a) Voskuhl, J.; Ravoo, B. J. *Chem. Soc. Rev.* **2008**, *38*, 495. (b) Nagle, J. F.; Tristram-Nagle, S. *Biochim. Biophys. Acta, Biomembr.* **2000**, *1469*, 159.
- (2) Bhattacharyya, K. *Acc. Chem. Res.* **2003**, *36*, 95.
- (3) Kunitake, T. *Angew. Chem., Int. Ed.* **1992**, *31*, 709.
- (4) Zimmerberg, J.; Gawrisch, K. *Nat. Chem. Biol.* **2006**, *2*, 564.
- (5) Ashgarian, N.; Schelly, Z. A. *Biochim. Biophys. Acta* **1999**, *1418*, 295.
- (6) Moyano, F.; Biasutti, M. A.; Silber, J. J.; Correa, N. M. *J. Phys. Chem. B* **2006**, *110*, 11838.
- (7) (a) Das, P.; Sarkar, D.; Chattopadhyay, N. *Chem. Phys. Lipid* **2008**, *158*, 38. (b) Sarkar, D.; Bose, D.; Mahato, A.; Ghosh, D.; Chattopadhyay, N. *J. Phys. Chem. B* **2010**, *114*, 2261.
- (8) Das, R.; Klymchenko, A. S.; Duportail, G.; Mely, Y. *J. Phys. Chem. B* **2008**, *112*, 11929.
- (9) Chaudhuri, S.; Pahari, B.; Sengupta, P. K. *Biophys. Chem.* **2009**, *139*, 29.
- (10) (a) Sujatha, J.; Mishra, A. K. *Langmuir* **1998**, *14*, 2256. (b) Mohapatra, M.; Subuddhi, U.; Mishra, A. K. *Photochem. Photobiol. Sci.* **2008**, *8*, 1373.
- (11) (a) Lakowicz, J. R. *Principles of Fluorescence Spectroscopy*; Plenum: New York, 1999. (b) *Topics in Fluorescence Spectroscopy*; Lakowicz, J. R., Ed.; Plenum Press: New York, 1994; Vol 2.
- (12) Mukherjee, S.; Chattopadhyay, A. *Langmuir* **2005**, *21*, 287.
- (13) Esquembre, R.; Ferrer, M. L.; Gutierrez, M. C.; Mallavia, R.; Mateo, C. R. *J. Phys. Chem. B* **2007**, *111*, 3665.
- (14) Weller, A. Z. *Elektrokhimiya* **1956**, *60*, 1144.
- (15) Heller, H. J.; Blattmann, H. R. *Pure Appl. Chem.* **1972**, *30*, 145.
- (16) Chou, P. T.; Martinez, M. L.; Clements, J. H. *Chem. Phys. Lett.* **1993**, *204*, 395.
- (17) (a) Chou, P. T.; McMorrow, D.; Aartsma, T. J.; Kasha, M. *J. Phys. Chem.* **1984**, *88*, 4596. (b) Park, S.; Kwon, O.-H.; Kim, S.; Park, S.; Choi, M.-G.; Cha, M.; Park, S. Y.; Jang, D.-J. *J. Am. Chem. Soc.* **2005**, *127*, 10070.
- (18) Warner, T.; Woessner, G.; Karmer, H. E. In *Photodegradation and Photostabilization of Coating*; Pappas, S. P.; Winglow, F. H.; Eds.; American Chemical Society: Washington, DC, 1981; Vol. 151, p 1.
- (19) Kim, S.; Seo, J.; Jung, H. K.; Kim, J.-J.; Park, S. Y. *Adv. Mater.* **2005**, *17*, 2077.
- (20) (a) Singh, R. B.; Mahanta, S.; Guchhait, N. *J. Photochem. Photobiol. B* **2008**, *91*, 1. (b) Singh, R. B.; Mahanta, S.; Guchhait, N. *Chem. Phys. Lett.* **2008**, *463*, 183.
- (21) (a) Das, R.; Mitra, S.; Nath, D.; Mukherjee, S. *J. Phys. Chem.* **1996**, *100*, 14514. (b) Abou-Zied, O. K. *J. Phys. Chem. B* **2007**, *111*, 9879. (c) Kamal, J. A. K.; Zhao, L.; Zewail, A. H. *Proc. Natl. Acad. Sci. U.S.A.* **2004**, *101*, 13411.
- (22) Klymchenko, A. S.; Shvadchak, V. V.; Yushchenko, D. A.; Jain, N.; Mely, Y. *J. Phys. Chem. B* **2008**, *112*, 12050.
- (23) Zhong, D.; Douhal, A.; Zewail, A. H. *Proc. Natl. Acad. Sci. U.S.A.* **2000**, *97*, 14056.
- (24) Roberts, E. L.; Chou, P. T.; Alexander, T. A.; Agbaria, R. A.; Warner, I. M. *J. Phys. Chem.* **1995**, *99*, 5431.
- (25) (a) Sarkar, N.; Das, N.; Das, S.; Datta, A.; Nath, D.; Bhattacharyya, K. *J. Phys. Chem.* **1995**, *90*, 17711. (b) Mukhopadhyay, M.; Banerjee, D.; Mukherjee, S. *J. Phys. Chem. A* **2006**, *110*, 12743.
- (26) Mukhopadhyay, M.; Mandal, A.; Misra, R.; Banerjee, D.; Bhattacharyya, S. P.; Mukherjee, S. *J. Phys. Chem. B* **2009**, *113*, 567.
- (27) Tielrooij, K. J.; Cox, M. J.; Bakker, H. J. *ChemPhysChem* **2009**, *10*, 245.
- (28) (a) Cohen, B.; Huppert, D.; Solnsteve, K. M.; Tsafadia, Y.; Nachliel, E.; Gutman, M. *J. Am. Chem. Soc.* **2002**, *124*, 7539. (b) Hashimoto, S.; Thomas, J. K. *J. Am. Chem. Soc.* **1985**, *107*, 4655, and references therein.
- (29) Paul, B. K.; Samanta, A.; Guchhait, N. *Langmuir* **2010**, *26*, 3214.
- (30) Singh, R. B.; Mahanta, S.; Kar, S.; Guchhait, N. *Chem. Phys.* **2007**, *331*, 373.
- (31) (a) Banerjee, D.; Srivastava, S. K.; Pal, S. K. *J. Phys. Chem. B* **2008**, *112*, 1828. (b) O'Connor, D. V.; Philips, D. *Time Correlated Single Photon Counting*; Academic Press: London, 1984.
- (32) Huang, C. *Biochemistry* **1969**, *8*, 344.
- (33) Frisch, M. J. *Gaussian 03*, Revision B.03; Gaussian, Inc.: Pittsburgh, PA, 2003.
- (34) (a) Morris, G. M.; Goodsell, D. S.; Halliday, R. S.; Huey, R.; Hart, W. E.; Belew, R. K.; Olson, A. J. *J. Comput. Chem.* **1998**, *19*, 1639. (b) Hetenyi, C.; van der Spoel, D. *FEBS Lett.* **2006**, *580*, 1447. (c) Bhattacharyya, B.; Nakka, S.; Guruprasad, L.; Samanta, A. *J. Phys. Chem. B* **2009**, *113*, 2143. (cc) Mulakala, C.; Nerinkx, W.; Reilly, P. J. *Carbohydr. Res.* **2007**, *342*, 163. (d) Maiti, T. K.; De, S.; Dasgupta, S.; Pathak, T. *Bioorg. Med. Chem.* **2006**, *14*, 1221. (e) Neelam, S.; Gokara, M.; Sudhamalla, B.; Amoora, D. G.; Subramanyam, R. *J. Phys. Chem. B* **2010**, *114*, 3005. (f) Holt, P. A.; Chaires, J. B.; Trent, J. O. *J. Chem. Inf. Model.* **2008**, *48*, 1602. (g) Morris, G. M.; Huey, R.; Lindstrom, W.; Sanner, M. F.; Belew, R. K.; Goodsell, D. S.; Olson, A. J. *J. Comput. Chem.* **2009**, *30*, 2785.
- (35) De Lano, W. L. *The PyMOL Molecular Graphics System*; De Lano Scientific: San Carlos, CA, 2002.
- (36) Rodrigues, C.; Gamerio, P.; Reis, S.; Lima, J. L. F. C.; Castro, B. D. *Langmuir* **2002**, *18*, 10231.
- (37) Mateo, C. R.; Douhal, A. *Proc. Natl. Acad. Sci. U.S.A.* **1998**, *95*, 7245.
- (38) Coutinho, A.; Prieto, M. *Biophys. J.* **1995**, *69*, 2541.
- (39) (a) Sengupta, B.; Banerjee, A.; Sengupta, P. K. *FEBS Lett.* **2004**, *570*, 77. (b) Sabin, J.; Prieto, G.; Russo, J. M.; Messina, P. V.; Salgado, F. J.; Nogueira, M.; Costas, M.; Sarmiento, F. *J. Phys. Chem. B* **2009**, *113*, 1655.
- (40) (a) Galley, W. C.; Purkey, P. M. *Proc. Natl. Acad. Sci. U.S.A.* **1970**, *67*, 1116. (b) Rubinov, A. N. *Tomin VI Opt. Spektr.* **1970**, *29*, 1082. (c) Weber, G.; Shinitzky, M. *Proc. Natl. Acad. Sci. U.S.A.* **1970**, *65*, 823.
- (41) (a) Demchenko, A. P. *Luminescence* **2002**, *17*, 19. (b) Mukherjee, S.; Chattopadhyay, A. *Langmuir* **1995**, *5*, 237. (c) Samanta, A. *J. Phys. Chem. B* **2006**, *110*, 13704, and references therein. (d) Gratzel, M.; Thomas, J. K. In *Modern Fluorescence Spectroscopy*; Wehrly, E. L., Ed.; Plenum Press: New York, 1976; Vol. 2.
- (42) (a) Singh, R. B.; Mahanta, S.; Bagchi, A.; Guchhait, N. *Photochem. Photobiol. Sci.* **2009**, *8*, 101. (b) Mahanta, S.; Singh, R. B.; Guchhait, N. *J. Fluoresc.* **2009**, *19*, 291.
- (43) Oldfield, E.; Chapman, D. *FEBS Lett.* **1972**, *23*, 285.
- (44) Chapman, E.; Williams, R. M.; Ladbrooke, B. D. *Chem. Phys. Lipids* **1967**, *1*, 445.
- (45) Trauble, H.; Haynes, D. H. *Chem. Phys. Lipids* **1971**, *7*, 324.
- (46) Lee, A. G.; Birdsall, N. J. M.; Levine, Y. K.; Metcaye, J. C. *Biochim. Biophys. Acta* **1972**, *255*, 43.
- (47) Hubbell, W. L.; McConnell, H. M. *J. Am. Chem. Soc.* **1971**, *93*, 314.

- (48) (a) Flynn, D. C.; Ramakroshna, G.; Yang, H.-B.; Northrop, B. H.; Stang, P. J.; Goodson, T., III *J. Am. Chem. Soc.* **2010**, *132*, 1348. (b) Wang, Y.; Clark, T. B.; Goodson, T., III *J. Chem. Phys. B* **2010**, *114*, 7112.
- (49) (a) Mallick, A.; Halder, B.; Maiti, S.; Bera, S. C.; Chattopadhyay, N. *J. Phys. Chem. B* **2005**, *109*, 14675. (b) Panda, M.; Behera, P. K.; Misra, B. K.; Behera, G. B. *J. Photochem. Photobiol. A* **1995**, *90*, 69.
- (50) (a) Bhattacharya, B.; Nakka, S.; Guruprasad, L.; Samanta, A. *J. Phys. Chem. B* **2009**, *113*, 2143, and references therein. (b) Jha, A.; Udgaoonkar, J. B.; Krishnamoorthy, G. *J. Mol. Biol.* **2009**, *393*, 735. (c) Ko, C. W.; Wei, Z.; Marsh, R. J.; Armoogum, D. A.; Nicolaou, N.; Bain, A. J.; Zhou, A.; Ying, L. *Mol. BioSyst.* **2009**, *5*, 1025. (d) Knutson, J. R.; Davenport, L.; Brand, L. *Biochemistry* **1986**, *25*, 1805. (e) Barkley, M. D.; Kowalczyk, A. A.; Brand, L. *J. Chem. Phys.* **1981**, *75*, 3581. (f) Smith, T. A.; Irwanto, M.; Haines, D. J.; Ghiggino, K. P.; Millar, D. P. *Colloid Polym. Sci.* **1998**, *276*, 1032. (g) Das, T. K.; Mazumdar, S. *Biophys. Chem.* **2000**, *86*, 15. (h) Ludescher, R. D.; Petting, L.; Hudson, S.; Hudson, B. *Biophys. Chem.* **1987**, *28*, 59, and references therein.
- (51) (a) Dutt, G. B. *J. Phys. Chem. B* **2004**, *108*, 3651. (b) Dutta Choudhury, S.; Kumbhakar, M.; Nath, S.; Pal, H. *J. Chem. Phys.* **2007**, *127*, 194901. (c) Das, P.; Mallick, A.; Chakrabarty, A.; Halder, B.; Chattopadhyay, N. *J. Chem. Phys.* **2006**, *125*, 44516. (d) Ahlls, T.; Sberman, O.; Hjelm, C.; Lindman, B. *J. Phys. Chem.* **1983**, *87*, 822. (e) Nery, H.; Sberman, O.; Canet, D.; Walderhaug, H.; Lindman, B. *J. Phys. Chem.* **1986**, *90*, 5802. (f) Mahata, A.; Sarkar, D.; Bose, D.; Ghosh, D.; Girigoswami, A.; Das, P.; Chattopadhyay, N. *J. Phys. Chem. B* **2010**, *113*, 7517.
- (52) Thirunavukkuarasu, S.; Jares-Erijman, E. A.; Jovin, T. M. *J. Mol. Biol.* **2008**, *378*, 1064.
- (53) (a) Zhao, G.-J.; Han, K.-L. *Biophys. J.* **2008**, *94*, 38. (b) Laine, R. M.; Sulaiman, S.; Brick, C.; Roll, M.; Tamaki, R.; Asuncion, M. Z.; Neurock, M.; Filhol, J.-S.; Lee, C.-Y.; Zhang, J.; Goodson III, T.; Ronchi, M.; Pizzotti, M.; Rand, S. C.; Li, Y. *J. Am. Chem. Soc.* **2010**, *132*, 3708. (c) Zhao, G.-J.; Chen, R.-K.; Sun, M.-T.; Liu, J.-Y.; Li, G.-Y.; Gao, Y.-L.; Han, K.-L.; Yang, X.-C.; Sun, L. *Chem.—Eur. J.* **2008**, *14*, 6935.
- (54) (a) Zhao, G.-J.; Liu, J.-Y.; Zhou, L.-C.; Han, K.-L. *J. Phys. Chem. B* **2007**, *111*, 8940. (b) Zhao, G.-J.; Han, K.-L. *J. Phys. Chem. A* **2007**, *111*, 9218. (c) Zhao, G.-J.; Han, K.-L. *J. Phys. Chem. A* **2009**, *113*, 14329. (d) Zhao, G.-J.; Han, K.-L. *J. Phys. Chem. A* **2007**, *111*, 2469. (e) Zhao, G.-J.; Han, K.-L. *ChemPhysChem* **2008**, *9*, 1842.
- (55) (a) Biczok, L.; Cser, A.; Nagy, K. *J. Photochem. Photobiol. A* **2001**, *146*, 59. (b) Miskolczy, Z.; Biczok, L.; Megyesi, M.; Jablonkai, I. *J. Phys. Chem. B* **2009**, *113*, 1645. (c) Biczok, L.; Berces, T.; Inoue, H. *J. Phys. Chem. A* **1999**, *103*, 3837. (d) Biczok, L.; Berces, T.; Yatsuhashi, T.; Tachibana, H.; Inoue, H. *Phys. Chem. Chem. Phys.* **2001**, *3*, 980.

JP1048138